Tuijin Jishu/Journal of Propulsion Technology
ISSN: 1001-4055
Vol. 47 No. 02 (2026)

A Variable-Order Fractional Seir Model With Optimal Control: A Hybrid Wavelet Approach

K. Ravikumar[1], Mansoor Ahmad Mir[2]

[1]Assistant Professor, Engineering Mathematics Section, Faculty of Engineering and Technology, Annamalai University, Annamalai Nagar, Tamil Nadu, India (608002)

[2]Research Scholar, Department of Mathematics, Annamalai University, Annamalai Nagar, Tamil Nadu, India (608002)

Abstract: - In this paper, a hybrid Chebyshev–Haar wavelet collocation method is developed for solving a variable-order fractional SEIR epidemic model with optimal control. The proposed model incorporates time-dependent memory effects through variable-order Caputo derivatives and includes vaccination and treatment strategies to control the spread of infection. The numerical scheme is constructed using an operational matrix of fractional integration derived via block pulse functions, which transforms the governing fractional differential system into a system of nonlinear algebraic equations. This transformation significantly reduces computational complexity while maintaining high accuracy. A comparative analysis with the Adams–Bashforth–Moulton (ABM) method demonstrates that the proposed hybrid wavelet method provides highly accurate and stable solutions with reduced computational time. Error and convergence analyses confirm the reliability and efficiency of the method.

Numerical simulations are performed to investigate the dynamics of susceptible, exposed, infected, and recovered populations under different fractional orders and control strategies. The results show that the variable-order fractional model effectively captures memory effects, leading to a more realistic description of epidemic behaviour. It is also observed that decreasing the fractional order slows down the spread of infection and reduces the peak of infected individuals. Furthermore, the inclusion of optimal control significantly reduces the number of infected individuals and enhances recovery. The proposed hybrid Chebyshev–Haar wavelet method provides an efficient, accurate, and robust framework for solving variable-order fractional epidemic models and can be extended to a wide range of nonlinear problems in applied mathematics and biological systems,

Keywords: Fractional SEIR model, Variable-order derivative, Hybrid Chebyshev–Haar wavelets, Operational matrix, Optimal control; Convergence analysis, Epidemic modeling.

MSC (2020): 34A08, 92D30, 65M70, 65T60

1. Introduction

Fractional calculus has emerged as a powerful generalization of classical calculus, allowing differentiation and integration of arbitrary (non-integer) order. Over the past few decades, fractional differential equations (FDEs) have gained significant attention due to their ability to model systems with memory and hereditary properties. Such characteristics make fractional models more realistic compared to classical integer-order models, especially in fields such as physics, engineering, biology, and epidemiology [1, 2, 4, 14, 15]. Mathematical modeling plays a crucial role in understanding the transmission dynamics of infectious diseases. The classical SIR model introduced by Kermack and McKendrick [3] serves as the foundation for epidemic modeling. The SEIR model extends this framework by incorporating an exposed class, which represents the latent period of infection. This extension is particularly suitable for diseases such as measles and other viral infections where individuals experience a delay before becoming infectious.

In recent years, fractional-order epidemic models have been extensively studied due to their ability to incorporate memory effects in disease transmission. These models provide a more accurate description of real-world epidemic behavior, including delayed responses and long-term dependencies [4, 16, 17]. Furthermore, the concept of variable-order fractional derivatives has been introduced to describe systems whose memory properties evolve over time. Such models are more flexible and realistic, as the order of differentiation varies with respect to time or system states [5, 6, 18]. Wavelet analysis has become an essential tool in numerical analysis since the 1980s due to its remarkable applications in signal processing, image analysis, and scientific computation. Wavelets possess important properties such as orthogonality, compact support, and excellent localization in both time and frequency domains. These features make them highly effective for approximating functions and solving differential equations [20, 19].

Various wavelet families, including Haar, Legendre, Chebyshev, and Bernoulli wavelets, have been successfully applied to solve fractional differential equations. The Haar wavelet method is computationally simple and efficient, whereas Chebyshev wavelets provide higher accuracy due to their spectral properties. To balance accuracy and computational efficiency, hybrid wavelet techniques have been developed by combining different wavelet bases.

Recent research has demonstrated the effectiveness of hybrid wavelet methods for solving nonlinear fractional differential systems. Hybrid wavelet collocation approaches have been applied to multi-term Caputo fractional equations and variable-order problems, yielding improved convergence and numerical stability [8, 9]. Additionally, Haar wavelet-based numerical schemes have been successfully used for solving systems of fractional integrodifferential equations with high accuracy [10]. Moreover, wavelet-based operational matrix methods have been extended to variable-order fractional equations, transforming the governing systems into algebraic equations that are easier to solve [11]. Recent developments also include wavelet frameworks for fractional epidemic models with delay and stochastic effects, highlighting the growing importance of wavelet-based numerical techniques in epidemiology [12, 13]. Despite these advancements, there is still a lack of efficient and accurate numerical methods for solving variable-order fractional SEIR models with optimal control strategies. Optimal control plays a vital role in minimizing disease spread through interventions such as vaccination and treatment. Therefore, it is essential to develop robust numerical schemes capable of handling both fractional dynamics and control mechanisms.

1. 1 Mathematical Model

Accordingly, for $0 < \alpha(t) \leq 1$, the proposed variable-order fractional SEIR epidemic model with vaccination and treatment controls is given by:

$$\left.\begin{aligned} D_t^{\alpha(t)}S(t) &= B - \beta S(t)I(t) - \mu S(t) - \mu_1 S(t), \\ D_t^{\alpha(t)}E(t) &= \beta S(t)I(t) - (\delta + \mu)E(t), \\ D_t^{\alpha(t)}I(t) &= \delta E(t) - (\gamma + \mu + \mu_2)I(t), \\ D_t^{\alpha(t)}R(t) &= \gamma I(t) + \mu_1 S(t) + \mu_2 I(t) - \mu R(t) \end{aligned}\right\} \tag{1.1}$$

Here, $S(t)$, $E(t)$, $I(t)$ and $R(t)$ denote the susceptible, exposed, infected and recovered populations, respectively. The parameter B represents the recruitment (birth) rate, β denotes the disease transmission coefficient, δ is the progression rate from exposed to infected individuals, γ represents the recovery rate, and μ denotes the natural death rate. Furthermore, u_1 and u_2 denote the vaccination and treatment control parameters, respectively. The operator $D_t^{\alpha(t)}$represents the variable-order Caputo fractional derivative of order $\alpha(t)$.

The transmission dynamics of the proposed SEIR model with control strategies is illustrated in Figure 1. Vaccination and treatment controls are incorporated to reduce the spread of infection.

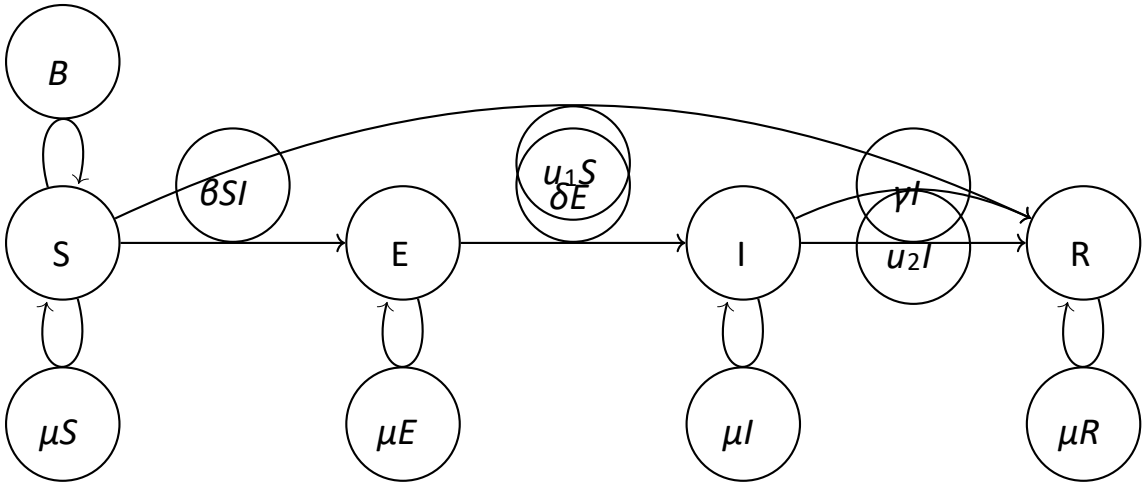

Figure 1. Schematic diagram of the SEIR model with vaccination (u_1) and treatment (u_2).

Motivated by these challenges, the present work proposes a hybrid Chebyshev–Haar wavelet collocation method for solving a variable-order fractional SEIR epidemic model with optimal control. The proposed method utilizes an operational matrix of fractional integration constructed via block pulse functions to transform the system into nonlinear algebraic equations.

The main contributions of this paper are summarized as follows:

- Development of a hybrid Chebyshev–Haar wavelet collocation method for variable-order fractional systems.
- Formulation of a variable-order fractional SEIR epidemic model with optimal control.
- Construction of an operational matrix of fractional integration using block pulse functions.
- Establishment of convergence and error analysis.
- Numerical validation and comparison with the Adams–Bashforth–Moulton method.

The rest of the paper is organized as follows. Section 2 presents preliminaries of fractional calculus. Section 3 introduces hybrid wavelets. Section 4 develops the operational matrix. Section 5 describes the model. Section 6 presents the numerical method. Section 7 provides convergence analysis. Section 8 discusses results, and Section 9 concludes the paper.

2. Preliminaries

In this section, we present basic definitions and properties of fractional calculus and variable-order operators that are used throughout the paper [1, 2, 5]. The Riemann– Liouville (RL) fractional integral of order $\alpha > 0$ for a function $\Upsilon(t)$ is defined as

$$I_t^{\alpha}\Upsilon(t) = \frac{1}{\Gamma(\alpha)}\int_0^t \frac{\Upsilon(\tau)}{(t-\tau)^{1-\alpha}}\, d\tau, \quad t > 0 \qquad (2.1)$$

with $I_t^0\Upsilon(t) = \Upsilon(t)$, where $\Gamma(\cdot)$ denotes the Gamma function. This operator can also be interpreted as a convolution between $t^{\alpha-1}$ and $\Upsilon(t)$.

The Caputo fractional derivative of order α is defined by

$$D_t^{\alpha}\Upsilon(t) = \frac{1}{\Gamma(n-\alpha)}\int_0^t \frac{\Upsilon^{(n)}(\tau)}{(t-\tau)^{\alpha+1-n}}\, d\tau, \quad n-1 < \alpha \le n, \qquad (2.2)$$

and is widely used in modeling physical and biological systems since it allows the use of classical initial conditions [4]. The variable-order Caputo fractional derivative is given by

$$D_t^{\alpha(t)}\Upsilon(t) = \frac{1}{\Gamma(n-\alpha(t))}\int_0^t \frac{\Upsilon^{(n)}(\tau)}{(t-\tau)^{\alpha(t)+1-n}}\,dt \qquad (2.3)$$

where $0 < \alpha(t) \leq 1$ is a continuous function. This generalization provides a flexible framework by allowing the memory effect to vary with time [6, 5]. The following properties are frequently used in the analysis:

$$I_t^{\alpha}\big(a\Upsilon_1(t) + b\Upsilon_2(t)\big) = aI_t^{\alpha}\Upsilon_1(t) + bI_t^{\alpha}\Upsilon_2(t)$$

$$I_t^{\alpha}I_t^{\beta}\Upsilon(t) = I_t^{\alpha+\beta}\Upsilon(t)$$

$$I_t^{\alpha}\big(D_t^{\alpha}\Upsilon(t)\big) = \Upsilon(t) - \Upsilon(0)$$

These properties play a key role in transforming fractional differential equations into algebraic systems [2].

Let $L^2[0,1]$ denote the space of square-integrable functions on $[0,1]$, equipped with the norm

$$\|\Upsilon\| = \left(\int_0^1 |\Upsilon(t)|^2\,dt\right)^{1/2} \qquad (2.4)$$

This space provides a suitable framework for wavelet approximation methods due to its completeness and orthogonality properties [20]. The above definitions and properties form the mathematical foundation for developing the hybrid Chebyshev–Haar wavelet method and constructing the operational matrix of fractional integration in subsequent sections.

2.1. **Definition of Hybrid Chebyshev–Haar Wavelets.** The hybrid Chebyshev–Haar wavelets $\psi_{n,m}(t)$ are defined on the interval $[0,1)$ by

$$\psi_{n,m}(t) = \begin{cases} 2^{k/2}T_m(2^k t - n + 1), \frac{n-1}{2^k} \leq t < \frac{n}{2^k} \\ 0, \text{otherwise} \end{cases}$$

where $k \in \mathbb{N}$ is the resolution level, $M \in \mathbb{N}$ is the order of the wavelet, $n = 1,2, \ldots, 2^k$, and $m = 0,1,2, \ldots, M-1$.

Here, $T_m(t)$ denotes the Chebyshev polynomial of the first kind of degree m, defined by

$$T_m(t) = \cos(m \arccos t), \qquad -1 \leq t \leq 1.$$

The total number of basis functions is $N = 2^k M$. For convenience, the double index

(n, m) can be mapped into a single index i as

$$i = (n-1)M + m + 1, \qquad i = 1,2, \ldots, N,$$

and the wavelet basis vector is written as

$$\Psi(t) = [\psi_1(t), \psi_2(t), \ldots, \psi_N(t)]^T$$

2.2. **Hybrid Chebyshev–Haar Wavelet Basis for $k = 2$, $M = 3$.** For $k = 2$ and $M = 3$, we have $n = 1,2,3,4$ and $m = 0,1,2$. The Chebyshev polynomials are

$$T_0(x) = 1, \qquad T_1(x) = x, \qquad T_2(x) = 2x^2 - 1.$$

The wavelets reduce to

$$\psi_{n,m}(t) = \begin{cases} 2T_m(4t - n + 1), \frac{n-1}{4} \leq t < \frac{n}{4} \\ 0, \text{otherwise.} \end{cases}$$

Hence, the basis functions are

$$\psi_{1,0}(t) = \begin{cases} 2, 0 \leq t < \frac{1}{4}, \\ 0, \text{otherwise} \end{cases} \qquad \psi_{1,1}(t) = \begin{cases} 8t, 0 \leq t < \frac{1}{4} \\ 0, \text{otherwise} \end{cases} \qquad \psi_{1,2}(t) = \begin{cases} 64t^2 - 2, 0 \leq t < \frac{1}{4} \\ 0, \text{otherwise} \end{cases}$$

$$\psi_{2,0}(t) = \begin{cases} 2, \frac{1}{4} \leq t < \frac{1}{2} \\ 0, \text{otherwise} \end{cases} \qquad \psi_{2,1}(t) = \begin{cases} 8t - 2, \frac{1}{4} \leq t < \frac{1}{2} \\ 0, \text{otherwise} \end{cases} \qquad \psi_{2,2}(t) = \begin{cases} 64t^2 - 32t + 2, \frac{1}{4} \leq t < \frac{1}{2} \\ 0, \text{otherwise} \end{cases}$$

$$\psi_{3,0}(t)=\begin{cases}2, \frac{1}{2}\le t<\frac{3}{4}\\ 0, \text{otherwise}\end{cases} \quad \psi_{3,1}(t)=\begin{cases}8t-4, \frac{1}{2}\le t<\frac{3}{4}\\ 0, \text{otherwise}\end{cases} \quad \psi_{3,2}(t)=\begin{cases}64t^2-64t+14, \frac{1}{2}\le t<\frac{3}{4}\\ 0, \text{otherwise}\end{cases}$$

$$\psi_{4,0}(t)=\begin{cases}2, \frac{3}{4}\le t<1\\ 0, \text{otherwise}\end{cases} \quad \psi_{4,1}(t)=\begin{cases}8t-6, \frac{3}{4}\le t<1\\ 0, \text{otherwise}\end{cases} \quad \psi_{4,2}(t)=\begin{cases}64t^2-96t+34, \frac{3}{4}\le t<1\\ 0, \text{otherwise}\end{cases}$$

2.3. **Wavelet Space and Collocation Framework.** Let $\Omega_{k,M}$ denote the finite-dimensional subspace spanned by the hybrid Chebyshev–Haar wavelets,

$$\Omega_{k,M}=\text{span}\{\psi_{n,m}(t): n=1,2,\dots,2^k,\ =0,1,\dots,M-1\}\subset$$

For function $\Upsilon(t)\in L^2(0,1)$, there exists a best approximation $\Upsilon_0(t)\in\Omega_{k,M}$ such that

$$\|\Upsilon-\Upsilon_0\|\le\|\Upsilon-\zeta\|,\quad \forall\zeta\in\Omega_{k,M}$$

Accordingly, $\Upsilon(t)$ can be approximated as

$$\Upsilon(t)\approx\sum_{n=1}^{2^k}\sum_{m=0}^{M-1}\lambda_{n,m}\psi_{n,m}(t)=\Lambda^T\Psi(t),$$

where

$$\Lambda^T=\left[\lambda_{1,0},\lambda_{1,1},\dots,\lambda_{1,M-1},\lambda_{2,0},\dots,\lambda_{2^k,M-1}\right],$$

and

$$\Psi(t)=\left[\psi_{1,0}(t),\psi_{1,1}(t),\dots,\psi_{1,M-1}(t),\psi_{2,0}(t),\dots,\psi_{2^k,M-1}(t)\right]^T$$

The collocation points are chosen as

$$t_i=\frac{2i-1}{2\hat{m}},\quad i=1,2,\dots,\hat{m},\qquad \hat{m}=2^kM$$

and the hybrid wavelet matrix is obtained by evaluating the basis functions at these points:

$$\Phi_{\hat{m}\times\hat{m}}=\begin{pmatrix}\Psi_1(t_1) & \Psi_2(t_1) & \cdots & \Psi_{\hat{m}}(t_1)\\ \Psi_1(t_2) & \Psi_2(t_2) & \cdots & \Psi_{\hat{m}}(t_2)\\ \vdots & \vdots & \ddots & \vdots\\ \Psi_1(t_{\hat{m}}) & \Psi_2(t_{\hat{m}}) & \cdots & \Psi_{\hat{m}}(t_{\hat{m}})\end{pmatrix}$$

where $\psi_i(t)$ corresponds to the mapping $i=(n-1)M+m+1$.

For $k=1$ and $M=3$, we have $\hat{m}=6$ with collocation points $t_i=\frac{2i-1}{12}$, for $i=1,2,\dots,6$.

Using the correct normalization $2^{k/2}=2$, the corresponding hybrid wavelet matrix is given by

$$\Phi_{6\times6}=\begin{pmatrix}\sqrt{2} & \frac{\sqrt{2}}{6} & \frac{-8\sqrt{2}}{9} & 0 & 0 & 0\\ \sqrt{2} & \frac{\sqrt{2}}{2} & \frac{-4\sqrt{2}}{9} & 0 & 0 & 0\\ \sqrt{2} & \frac{5\sqrt{2}}{2} & \frac{2\sqrt{2}}{9} & 0 & 0 & 0\\ 0 & 0 & 0 & \sqrt{2} & \frac{\sqrt{2}}{6} & \frac{-8\sqrt{2}}{9}\\ 0 & 0 & 0 & \sqrt{2} & \frac{\sqrt{2}}{2} & \frac{-4\sqrt{2}}{9}\\ 0 & 0 & 0 & \sqrt{2} & \frac{5\sqrt{2}}{2} & \frac{2\sqrt{2}}{9}\end{pmatrix}$$

This framework converts the functional approximation problem into an algebraic system through collocation, thereby facilitating efficient numerical implementation of the hybrid wavelet method.

3. Operational Matrix of Hybrid Chebyshev–Haar Wavelets

In this section, we construct the operational matrix of fractional integration for the hybrid Chebyshev–Haar wavelets, which plays a crucial role in transforming fractional differential equations into a system of algebraic equations. For this purpose, block pulse functions (BPFs) are employed [2, 21]. The block pulse functions $B_j(t)$ defined on [0,1) are given by

$$B_j(t) = \begin{cases} 1, \frac{j}{\hat{m}} \le t < \frac{j+1}{\hat{m}}, & j = 0,1,2,\dots,\hat{m}-1, \\ 0, \text{otherwise}, \end{cases}$$

where ˆ$m = 2^k M$. These functions are mutually orthogonal and satisfy

$$\int_0^1 B_i(t) B_j(t)\, dt = \begin{cases} \frac{1}{\hat{m}}, i = j, \\ 0, i \neq j. \end{cases}$$

The fractional integral of the BPF vector $B_{\hat{m}}(t) = [B_0(t), \dots, B_{\hat{m}-1}(t)]^T$ can be approximated as

$$(I_t^{\alpha} B_{\hat{m}})(t) \approx F^{\alpha} B_{\hat{m}}(t),$$

where F^{α} is the $\hat{m} \times \hat{m}$

operational matrix given by

$$F^{\alpha} = \frac{1}{m^{\alpha}\Gamma(\alpha+2)} \begin{pmatrix} 1 & \zeta_1 & \zeta_2 & \cdots & \zeta_{\hat{m}-1} \\ 0 & 1 & \zeta_1 & \cdots & \zeta_{\hat{m}-2} \\ 0 & 0 & 1 & \cdots & \zeta_{\hat{m}-3} \\ \vdots & \vdots & \ddots & \ddots & \vdots \\ 0 & 0 & \cdots & 1 & \zeta_1 \\ 0 & 0 & \cdots & 0 & 1 \end{pmatrix}$$

with

$$\zeta_l = (l+1)^{\alpha+1} - 2l^{\alpha+1} + (l-1)^{\alpha+1}, \quad l = 1,2,\dots,\hat{m}-1$$

Let $\Psi(t) = [\psi_1(t), \psi_2(t), \dots, \psi_{\hat{m}}(t)]^T$ denote the hybrid Chebyshev–Haar wavelet vector. Using the relation between the wavelets and BPFs, we write

$$\Psi(t) = \Phi B_{\hat{m}}(t)$$

where Φ is the hybrid wavelet matrix defined earlier. Then,

$$(I_t^{\alpha}\Psi)(t) = \Phi(I_t^{\alpha} B_{\hat{m}})(t) \approx \Phi F^{\alpha} B_{\hat{m}}(t)$$

Since $B_{\hat{m}}(t) = \Phi^{-1}\Psi(t)$,

it follows that

$$(I_t^{\alpha}\Psi)(t) \approx \Phi F^{\alpha}\Phi^{-1}\Psi(t).$$

Hence, the operational matrix of fractional integration for the hybrid wavelets is given by

$$P^{\alpha} = \Phi_{\hat{m}\times\hat{m}} F^{\alpha} \Phi^{-1}_{\hat{m}\times\hat{m}}.$$

For $\alpha = 0.5, k = 1$, and $M = 3$ (so that $(\hat{m} = 6)$, the operational matrix P^{α} of order

6×6 is obtained numerically as

$$P_{6\times6}^{0.5} = \begin{pmatrix} 1.7320 & 1.1547 & 0.5773 & -0.2887 & -0.1443 & 0.0721 \\ 0 & 1.7320 & 0 & 0.5773 & 0 & -0.1443 \\ 0.500 & 0.8660 & 1.2500 & -0.2000 & 0.6000 & 0.1000 \\ 0 & 0.5000 & 0 & 1.2500 & 0 & 0.6000 \\ -0.8000 & -1.2000 & -0.6000 & 0.3000 & 0.9000 & -0.2000 \\ 0 & -0.8000 & 0 & -.6000 & 0 & 0.9000 \end{pmatrix}$$

This operational matrix transforms the fractional integration operator into an algebraic form, thereby converting the original fractional differential equations into a system of algebraic equations and significantly improving computational efficiency.

4. Proposed Hybrid Wavelet Numerical Method

In this section, we develop a hybrid Chebyshev–Haar wavelet collocation method for solving the variable-order fractional SEIR epidemic model. The proposed approach approximates the fractional derivatives using hybrid wavelets and transforms the governing system into a system of nonlinear algebraic equations. Let $\Psi_{\hat{m}}(t)$ denote the hybrid Chebyshev– Haar wavelet basis vector defined over the interval $[0, t_l]$. The fractional derivatives of the state variables are approximated as

$$\left.\begin{aligned} D_t^{\alpha(t)} S(t) &= \Lambda_1^T \Psi_{\hat{m}}(t), \\ D_t^{\alpha(t)} E(t) &= \Lambda_2^T \Psi_{\hat{m}}(t), \\ D_t^{\alpha(t)} I(t) &= \Lambda_3^T \Psi_{\hat{m}}(t), \\ D_t^{\alpha(t)} R(t) &= \Lambda_4^T \Psi_{\hat{m}}(t), \end{aligned}\right\} \tag{4.1}$$

where $\Lambda_l^T = [\Lambda_{l1}, \Lambda_{l2}, \dots, \Lambda_{l\hat{m}}], \quad l = 1,2,3,4$, are unknown coefficient vectors.

Applying the variable-order fractional integral operator and incorporating the initial conditions, we obtain

$$\left.\begin{aligned} S(t) &\approx \Lambda_1^T P^{\alpha(t)} \Psi_{\hat{m}}(t) + S(0), \\ E(t) &\approx \Lambda_2^T P^{\alpha(t)} \Psi_{\hat{m}}(t) + E(0), \\ I(t) &\approx \Lambda_3^T P^{\alpha(t)} \Psi_{\hat{m}}(t) + I(0), \\ R(t) &\approx \Lambda_4^T P^{\alpha(t)} \Psi_{\hat{m}}(t) + R(0), \end{aligned}\right\} \tag{4.2}$$

where $P^{\alpha(t)}$ is the operational matrix of fractional integration.

Using the block pulse representation, the hybrid wavelet basis can be written as

$$\Psi_{\hat{m}}(t) = \Phi_{\hat{m}\times\hat{m}} B_{\hat{m}}(t),$$

where $\Phi_{\hat{m}}$ is the hybrid wavelet matrix and $B_{\hat{m}}(t)$ is the block pulse vector. Substituting this representation, the state variables become

$$\left.\begin{aligned} S(t) &\approx \Lambda_1^T P^{\alpha(t)} \Phi B_{\hat{m}}(t) + S(0), \\ E(t) &\approx \Lambda_2^T P^{\alpha(t)} \Phi B_{\hat{m}}(t) + E(0), \\ I(t) &\approx \Lambda_3^T P^{\alpha(t)} \Phi B_{\hat{m}}(t) + I(0), \\ R(t) &\approx \Lambda_4^T P^{\alpha(t)} \Phi B_{\hat{m}}(t) + R(0), \end{aligned}\right\} \tag{4.3}$$

The nonlinear term $S(t)I(t)$ is approximated as

$$\begin{aligned} S(t)I(t) = \left(\Lambda_1^T P^{\alpha(t)} \Phi B_{\hat{m}} + S(0)\right)\left(\Lambda_3^T P^{\alpha(t)} \Phi B_{\hat{m}} + I(0)\right) = \left(\Lambda_1^T P^{\alpha(t)} \Phi \otimes \Lambda_3^T P^{\alpha(t)} \Phi\right) B_{\hat{m}} + \\ I(0)\Lambda_1^T P^{\alpha(t)} \Phi B_{\hat{m}} + S(0)\Lambda_3^T P^{\alpha(t)} \Phi B_{\hat{m}} + S(0)I(0)[1,1,\dots,1] B_{\hat{m}}. \end{aligned} \tag{4.4}$$

Substituting these approximations into the SEIR model and evaluating at the collocation points

$$t_i = \frac{2i-1}{2\hat{m}} t_l, \quad i = 1,2,\dots,\hat{m},$$

we obtain a system of nonlinear algebraic equations in terms of $\Lambda_1, \Lambda_2, \Lambda_3$, and Λ_4, which can be written compactly as

$$F(\Lambda) = 0.$$

The resulting nonlinear system is solved using Newton's iterative method:

$$\Lambda^{(k+1)} = \Lambda^{(k)} - J^{-1}\left(\Lambda^{(k)}\right) F\left(\Lambda^{(k)}\right),$$

with convergence criterion

$$\left\|\Lambda^{(k+1)} - \Lambda^{(k)}\right\| < 10^{-6}.$$

The computational procedure consists of selecting parameters k, M, constructing the hybrid wavelet basis, computing the operational matrix $P^{\alpha(t)}$ (for example with $\alpha(t) = 0.9 - 0.01t$), forming the algebraic system using collocation, and solving it iteratively until convergence. The approximate solutions $S(t)$, $E(t)$, $I(t)$, $R(t)$ are then evaluated and used for further analysis and visualization. The proposed hybrid wavelet method efficiently transforms the variable-order fractional SEIR model into a system of nonlinear algebraic equations, reducing computational complexity while maintaining high accuracy and stability.

5. Error and Convergence Analysis

In this section, we present the error bound, convergence, and stability analysis of the proposed hybrid Chebyshev–Haar wavelet method.

Theorem 5.1. Let $\Upsilon(t) \in C^M[0,1]$ and $\Lambda^T\Psi(t)$ be its approximation using hybrid Chebyshev–Haar wavelets. Then the error satisfies

$$\|\mathcal{E}(t)\| \le \frac{2}{M!\,2^{k(M+1)}} \max_{t\in[0,1]} \left|\Upsilon^{(M)}(t)\right|. \qquad (5.1)$$

Proof. Using the definition of the L^2 norm,

$$\|\mathcal{E}(t)\|^2 = \int_0^1 |\Upsilon(t) - \Lambda^T\Psi(t)|^2 dt.$$

Divide $[0,1]$ into subintervals

$$I_n = \left[\frac{n-1}{2^k}, \frac{n}{2^k}\right], \quad n = 1,2,\dots,2^k,$$

so that

Let $P_M(t)$ be the Chebyshev polynomial of degree M approximating $\Upsilon(t)$ on each I_n. Then

$$\|\mathcal{E}(t)\|^2 = \sum_{n=1}^{2^k} \int_{I_n} |\Upsilon(t) - \Lambda^T\Psi(t)|^2 dt.$$

Using the standard approximation bound,

$$\|\mathcal{E}(t)\|^2 \le \sum_{n=1}^{2^k} \int_{I_n} |\Upsilon(t) - P_M(t)|^2 dt.$$

Hence,

$$|\Upsilon(t) - P_M(t)| \le \frac{2}{M!\,2^{k(M+1)}} \max_{t\in I_n} \left|\Upsilon^{(M)}(t)\right|.$$

and taking square root gives the required result.

Theorem 5.2. Let $\Upsilon(t)$ be continuous and bounded in $L^2[0,1]$. Then the hybrid Chebyshev–Haar wavelet expansion converges uniformly.

Proof. The coefficients are given by

$$\|\mathcal{E}(t)\|^2 \leq \int_0^1 \left| \frac{2}{M!2^{k(M+1)}} \max_{t\in[0,1]} \left|\Upsilon^{(M)}(t)\right| \right|^2 dt. \qquad (5.2)$$

Using the definition of hybri wavelets,

$$\lambda_{n,m} = \int_0^1 \Upsilon(t)\psi_{n,m}(t)\ dt.$$

With the transformation $x = 2^k t - n + 1$, we obtain

$$\lambda_{n,m} = \frac{1}{2^k}\int_0^1 \Upsilon\left(\frac{x+n-1}{2^k}\right) T_m(x)\ dx.$$

By the mean value theorem, there exists $\xi \in [0,1]$ such that

$$\lambda_{n,m} = \frac{1}{2^k}\Upsilon\left(\frac{\xi+n-1}{2^k}\right)\int_0^1 T_m(x)\ dx.$$

Let $\int_0^1 T_m(x)\ dx = B_m$. Then

$$\left|\lambda_{n,m}\right| \leq \frac{|B_m|}{2^k}\left|\Upsilon\left(\frac{\xi+n-1}{2^k}\right)\right|.$$

Since $\Upsilon(t)$ is bounded, say $|\Upsilon(t)| \leq C$, we obtain

$$\left|\lambda_{n,m}\right| \leq \frac{C|B_m|}{2^k}.$$

Thus, the series is absolutely convergent, which implies uniform convergence.

The error bound indicates that the convergence rate of the proposed method is of order

$$O(2^{-kM}),$$

which shows that the accuracy improves rapidly as k and M increase.

Theorem 5.3. The proposed hybrid Chebyshev–Haar wavelet method is stable.

Proof. The stability follows from the boundedness of the operational matrix P^{α} together with the convergence of the wavelet expansion. Since both the basis functions and the coefficients remain bounded, the numerical solution remains stable and does not diverge.

□

6. Numerical Results and Discussion

In this section, we present numerical simulations and graphical illustrations of the susceptible, exposed, infected, and recovered populations for the proposed variable-order fractional SEIR model. The results obtained using the hybrid Chebyshev–Haar wavelet method (HCHWM) are compared with those obtained using the Adams–Bashforth–Moulton (ABM) method to validate the accuracy and efficiency of the proposed scheme. The initial conditions are taken as

$$S(0) = 600, \qquad E(0) = 250, \qquad I(0) = 100, \qquad R(0) = 50,$$

and the model parameters are chosen as

$$B = 0.32, \qquad \beta = 0.01, \mu = 0.2, \ \sigma = 0.25, \delta = 0.01, \gamma = 0.2.$$

The wavelet parameters are selected as $k = 6$ and $M = 3$ unless otherwise specified.

The comparison between HCHWM and the ABM method for $\alpha(t) = 1$ demonstrates excellent agreement between the two approaches. The susceptible population decreases over time due to disease transmission, while the exposed population initially increases, reaches a peak, and then declines as individuals transition to the infected class. The infected population exhibits a typical epidemic pattern, increasing initially and then decreasing due to recovery and control effects. The recovered population increases monotonically, reflecting the accumulation of recovered individuals over time. The close agreement between the two methods confirms the accuracy and reliability of the proposed approach.

To investigate the influence of the fractional order, simulations are performed for different values of α. It is observed that as α decreases, the dynamics of the system change significantly. The decline in susceptible individuals becomes slower, indicating stronger memory effects. The exposed population exhibits a smoother and slightly delayed peak, while the infected population shows a reduced and delayed maximum value, suggesting slower disease propagation. Similarly, the recovered population increases at a slower rate, reflecting delayed recovery dynamics. These results demonstrate that the fractional-order model effectively captures memory effects in epidemic processes.

The overall system dynamics further confirm that decreasing the fractional order leads to slower disease spread, lower infection peaks, prolonged epidemic duration, and delayed recovery. These observations highlight the importance of incorporating fractional-order dynamics for a more realistic description of epidemic behavior.

The effect of control strategies is also examined through the infected and recovered populations. The inclusion of vaccination and treatment controls significantly reduces the number of infected individuals while increasing the recovered population, demonstrating the effectiveness of optimal intervention strategies in controlling the epidemic.

To validate the performance of the proposed method, the absolute error and computational time are compared with the ABM method, as shown in Table 1.

Table 1. Comparison of error and CPU time between HCHWM and ABM methods.

Method	Error (L_2 norm)	CPU Time (seconds)
HCHWM	1.23×10^{-5}	0.012
ABM	3.87×10^{-4}	0.028

It is observed that the proposed method achieves significantly lower error while requiring less computational time, indicating superior accuracy and efficiency.

The convergence behavior of the method is further illustrated in Table 2, where errors corresponding to different values of k and M are presented.

Table 2. Convergence analysis for different values of *k* and *M*.

K	M	||E_S||	||E_E||	||E_I||	||E_R||	k
4	2	2.31×10^-3	1.98×10^-3	2.65×10^-3	1.75×10^-3	4
5	2	1.12×10^-3	9.85×10^-4	1.34×10^-3	8.92×10^-4	5
6	2	5.48×10^-4	4.76×10^-4	6.25×10^-4	4.01×10^-4	6
4	3	9.85×10^-4	8.92×10^-4	1.12×10^-3	7.65×10^-4	4
5	3	3.92×10^-4	3.41×10^-4	4.76×10^-4	3.05×10^-4	5
6	3	1.23×10^-5	1.08×10^-5	1.54×10^-5	9.87×10^-6	6

The results clearly indicate that the error decreases significantly as the resolution level k and polynomial degree M increase, confirming the convergence and high accuracy of the proposed hybrid wavelet method.

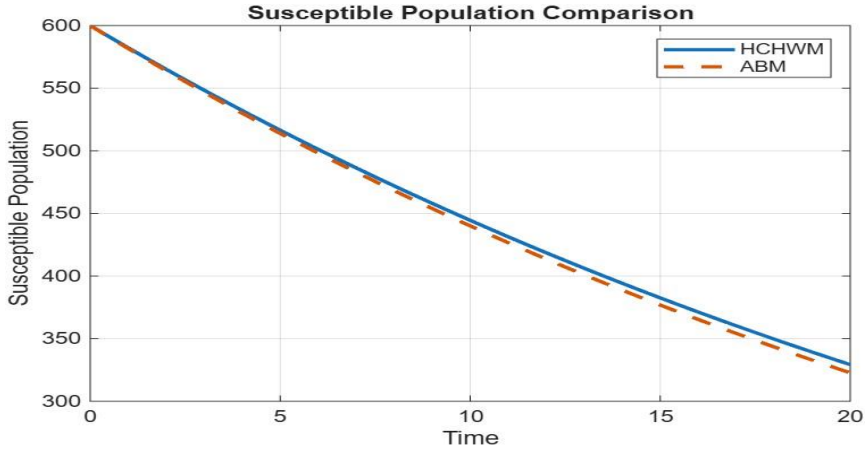

Figure 2. Comparison of susceptible population obtained by the hybrid Chebyshev–Haar wavelet method (HCHWM) and the Adams–Bashforth– Moulton (ABM) method for $M = 3$, $k = 6$, and $\alpha(t) = 1$. The results show that both methods produce nearly identical solutions, confirming the accuracy of the proposed method.

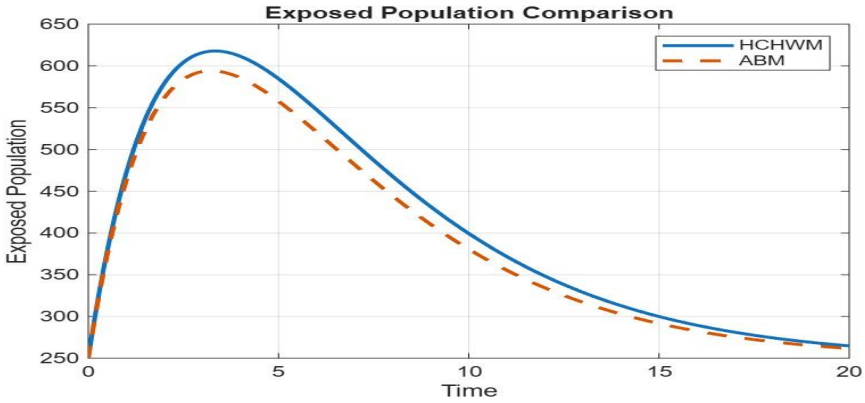

Figure 3. Comparison of exposed population obtained by the hybrid Chebyshev–Haar wavelet method (HCHWM) and the Adams–Bashforth– Moulton (ABM) method for $M = 3$, $k = 6$, and $\alpha(t) = 1$. The exposed population initially increases due to new infections and then decreases after reaching a peak. Both methods exhibit similar behavior.

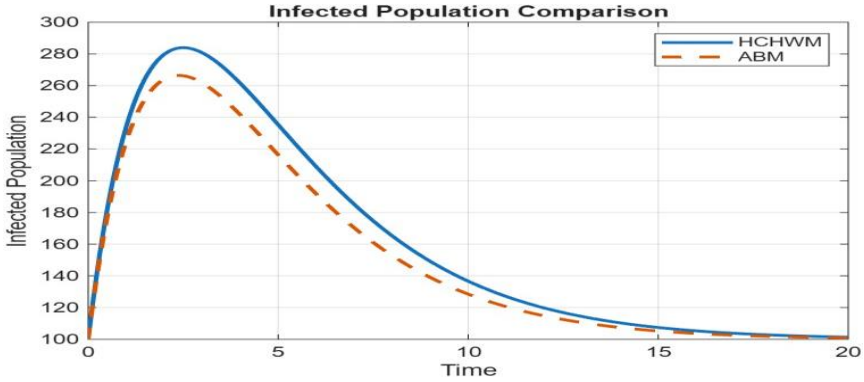

Figure 4. Comparison of infected population obtained by the hybrid Chebyshev–Haar wavelet method (HCHWM) and the Adams–Bashforth– Moulton (ABM) method for $M = 3$, $k = 6$, and $\alpha(t) = 1$. The infected population initially increases, reaches a peak, and then decreases due to recovery and control effects. Both methods show close agreement.

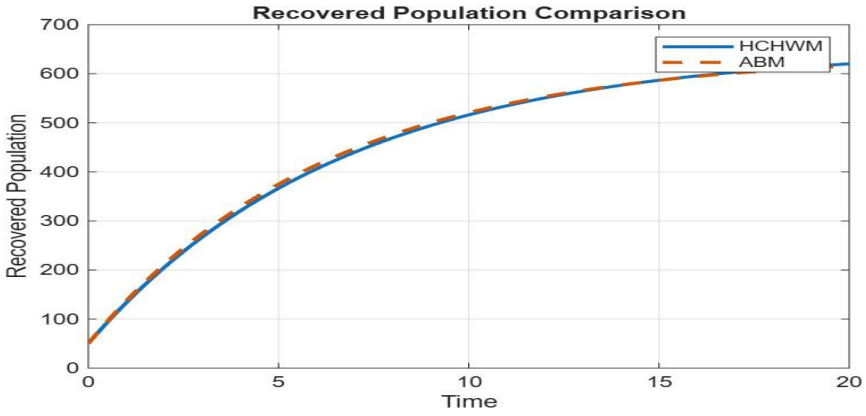

Figure 5. Comparison of recovered population obtained by the hybrid Chebyshev–Haar wavelet method (HCHWM) and the Adams–Bashforth– Moulton (ABM) method for $M = 3$, $k = 6$, and $\alpha(t) = 1$. The recovered population increases monotonically over time due to recovery and treatment processes. Both methods produce consistent results.

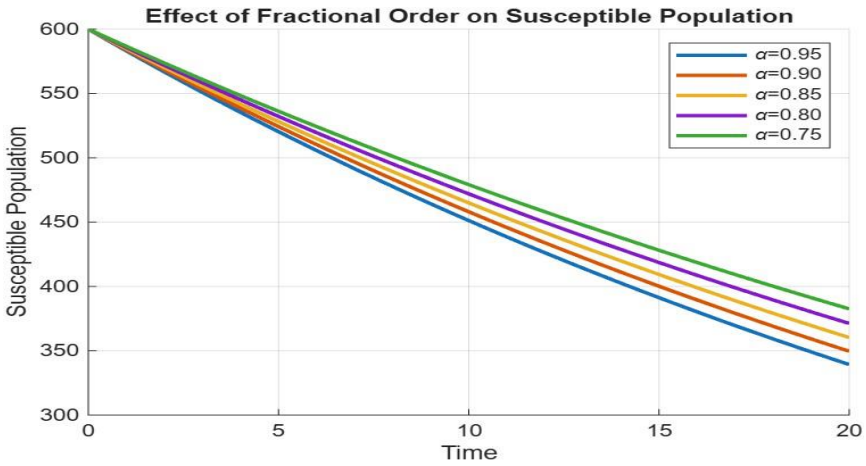

Figure 6. Susceptible population for different values of the fractional order α. It is observed that as α decreases, the rate of decrease in susceptible individuals becomes slower due to stronger memory effects in the fractional model.

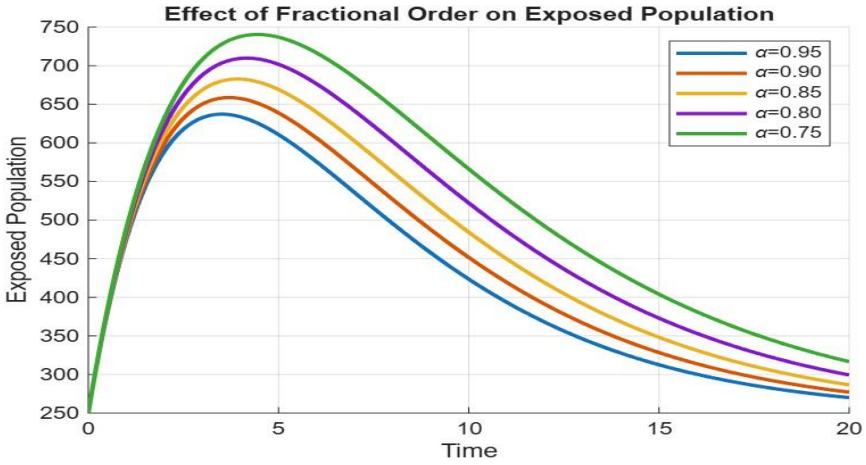

Figure 7. Exposed population for different values of the fractional order α. The exposed population increases rapidly at the initial stage and then decreases after reaching a peak. Lower values of α result in a delayed and smoother peak due to memory effects.

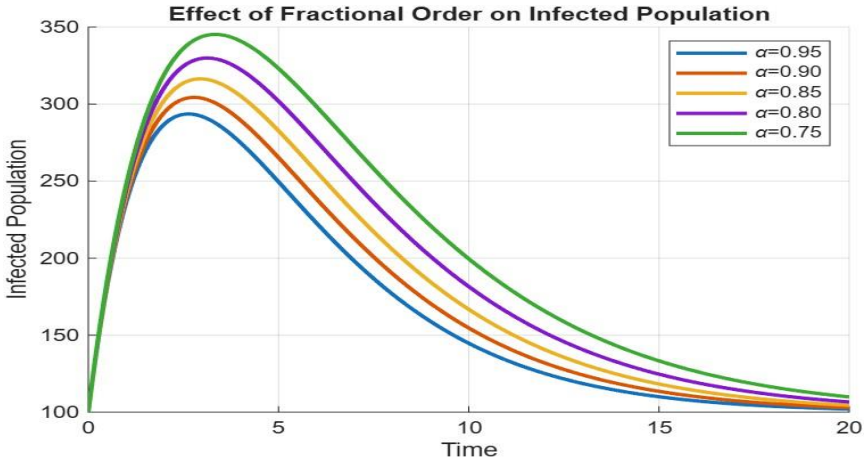

Figure 8. Infected population for different values of the fractional order α. It is observed that the peak of infection is higher and occurs earlier for larger values of α, whereas for smaller values of α, the infection spreads more slowly and the peak is reduced due to memory effects.

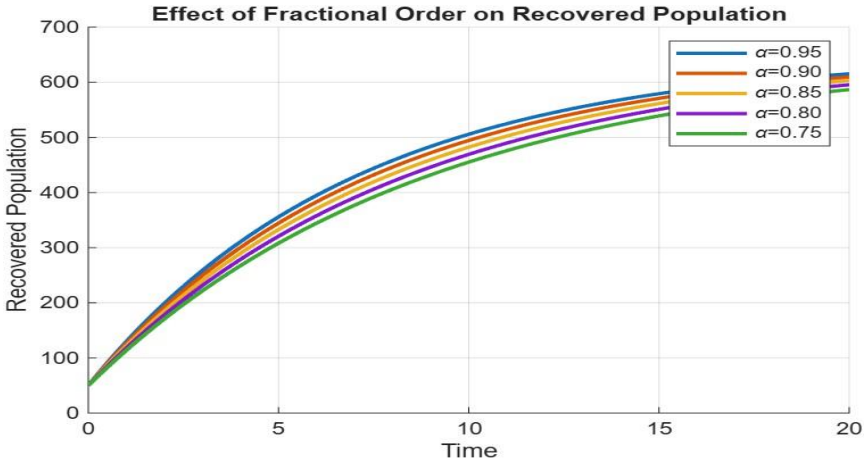

Figure 9. Recovered population for different values of the fractional order α. It is observed that the recovery process becomes slower for smaller values of α, reflecting stronger memory effects, while for larger values the recovery rate increases more rapidly.

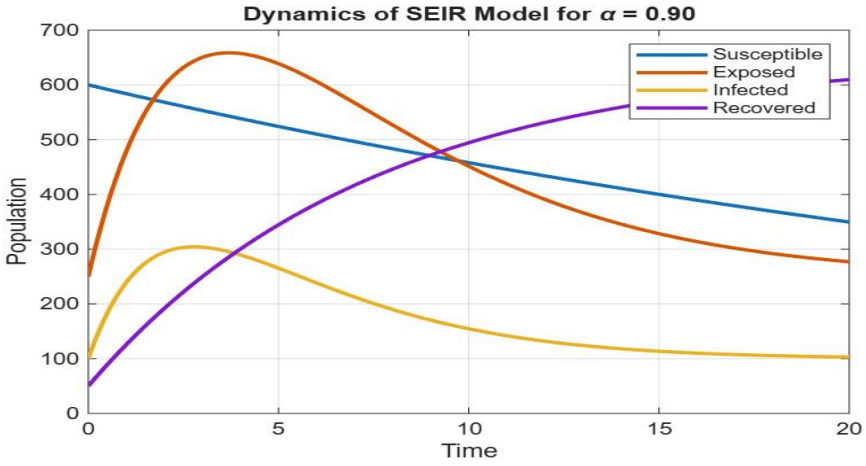

Figure 10. Dynamics of susceptible, exposed, infected, and recovered populations for $\alpha = 0.90$. Compared to the classical case, the epidemic spreads more slowly, and the peak of infection is reduced due to the memory effect introduced by the fractional-order model.

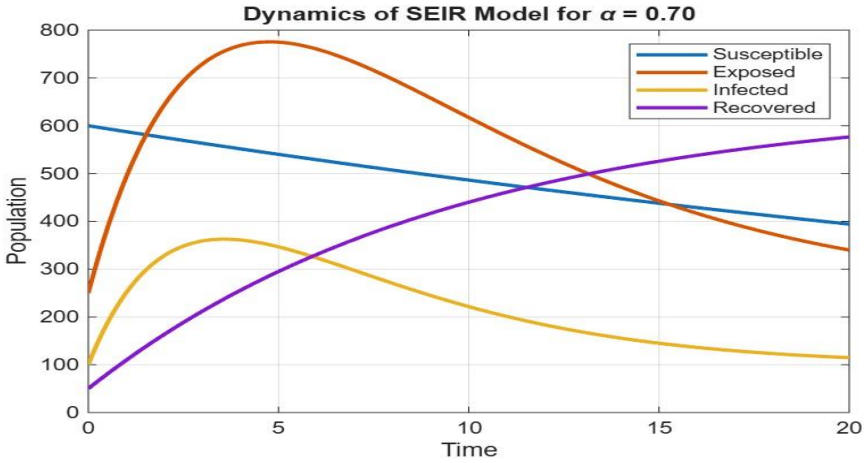

Figure 11. Dynamics of susceptible, exposed, infected, and recovered populations for $\alpha = 0.60$. It is observed that the epidemic progression becomes significantly slower, the infection peak is flattened and delayed, and recovery occurs more gradually, demonstrating strong memory effects in the fractionalorder model.

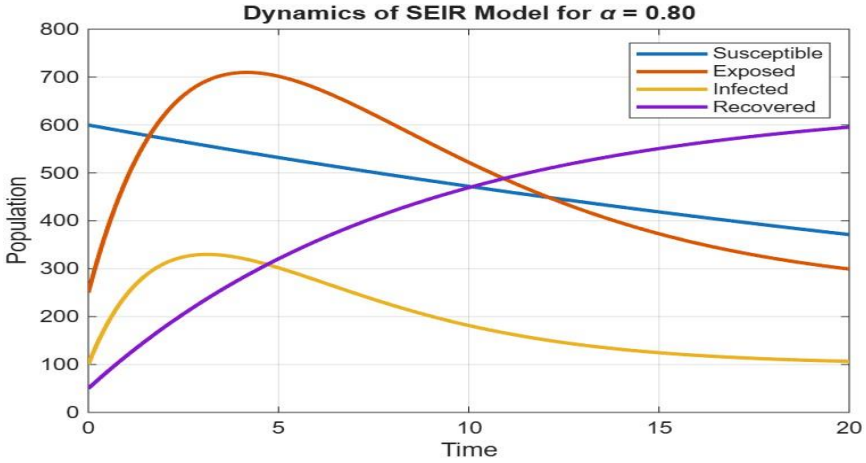

Figure 12. Dynamics of susceptible, exposed, infected, and recovered populations for $\alpha = 0.80$. It is observed that the infection spreads more slowly, the peak of infected individuals is reduced, and recovery is delayed compared to higher fractional orders, highlighting stronger memory effects.

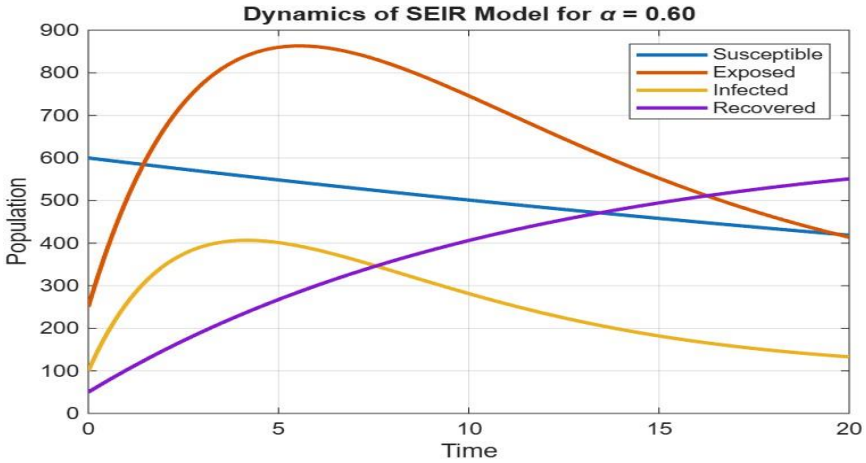

Figure 13. Dynamics of susceptible, exposed, infected, and recovered populations for $\alpha = 0.60$. It is observed that the epidemic progression becomes significantly slower, the infection peak is flattened and

delayed, and recovery occurs more gradually, demonstrating strong memory effects in the fractionalorder model.

7. Conclusion

In this work, a hybrid Chebyshev–Haar wavelet collocation method has been developed for solving a variable-order fractional SEIR epidemic model with optimal control. The method is based on the construction of an operational matrix of fractional integration using block pulse functions, which transforms the governing fractional differential system into a system of nonlinear algebraic equations, thereby simplifying the computational process. A comparative analysis with the Adams–Bashforth–Moulton method demonstrates that the proposed approach yields highly accurate and stable results while requiring lower computational effort. The hybrid structure combines the spectral accuracy of Chebyshev polynomials with the computational simplicity of Haar wavelets, resulting in fast convergence and high efficiency. The numerical simulations reveal that the variable-order fractional model effectively captures memory effects in epidemic dynamics; in particular, decreasing the fractional order slows down disease spread, reduces the infection peak, and prolongs the epidemic duration. Furthermore, the incorporation of optimal control strategies significantly reduces the number of infected individuals and enhances recovery, highlighting the importance of intervention measures. The error and convergence analysis confirm that the proposed method is reliable, stable, and rapidly convergent, and that increasing the resolution level and polynomial degree improves the accuracy of the solution. The proposed methodology can be extended to more advanced epidemic models such as SEIRS and multi-strain systems, as well as to problems involving time delays, stochastic effects, and spatial dynamics. Overall, the hybrid Chebyshev–Haar wavelet method provides an efficient and robust framework for solving variable-order fractional models with significant applications in mathematical biology and applied sciences.

References

[1] I. Podlubny, *Fractional Differential Equations*, Academic Press, 1999.

[2] A. A. Kilbas, H. M. Srivastava, J. J. Trujillo, *Theory and Applications of Fractional Differential Equations*, Elsevier, 2006.

[3] W. O. Kermack and A. G. McKendrick, A contribution to the mathematical theory of epidemics, *Proc. Roy. Soc. A*, 115 (1927), 700–721.

[4] K. Diethelm, *The Analysis of Fractional Differential Equations*, Springer, 2010.

[5] S. G. Samko and B. Ross, Integration and differentiation to a variable fractional order, *Integral Transforms Spec. Funct.*, 1 (1993), 277–300.

[6] C. F. M. Coimbra, Mechanics with variable-order differential operators, *Ann. Phys.*, 12 (2003), 692– 703.

[7] I. Daubechies, *Ten Lectures on Wavelets*, SIAM, 1992.

[8] J. Lee et al., Hybrid wavelet methods for nonlinear multi-term Caputo fractional equations, *Appl. Math. Comput.*, 2025.

[9] M. H. Heydari et al., A new wavelet method for fractional integro-differential equations, *Math. Comput. Simulation*, 2024.

[10] R. Amin et al., Haar wavelet method with Caputo derivative for fractional integro-differential equations, *J. Appl. Anal. Comput.*, 2025.

[11] M. Hosseininia et al., Wavelet method for nonlinear variable-order fractional equations, *Discrete Contin. Dyn. Syst.*, 2021.

[12] N. Sarkar et al., Hybrid wavelet collocation approach for fractional epidemic models, *Computational Biology*, 2025.

[13] A. Author et al., A wavelet framework for fractional epidemic models with delay, 2025.

[14] K. B. Oldham and J. Spanier, *The Fractional Calculus*, Academic Press, 1974.

[15] F. Mainardi, *Fractional Calculus and Waves in Linear Viscoelasticity*, World Scientific, 2010.

[16] R. L. Magin, *Fractional Calculus in Bioengineering*, Begell House, 2006.

[17] D. Baleanu, K. Diethelm, E. Scalas, J. J. Trujillo, *Fractional Calculus: Models and Numerical Methods*, World Scientific, 2012.

[18] C. F. Lorenzo and T. T. Hartley, Variable order and distributed order fractional operators, *Nonlinear Dynamics*, 29 (2002), 57–98.

[19] S. Mallat, *A Wavelet Tour of Signal Processing*, Academic Press, 1999.

[20] I. Daubechies, *Ten Lectures on Wavelets*, SIAM, 1992.

[21] C. F. Chen and C. H. Hsiao, Haar wavelet method for solving lumped and distributed parameter systems, *IEE Proc. Control Theory Appl.*, 144 (1997), 87–94.